



ELSEVIER

Colloids and Surfaces A: Physicochem. Eng. Aspects xxx (2004) xxx–xxx

COLLOIDS  
AND  
SURFACES

A

www.elsevier.com/locate/colsurfa

# Evolution of water-in-oil emulsion controlled by droplet-bulk ion exchange: acoustic, electroacoustic, conductivity and image analysis

A. Dukhin\*, P. Goetz

*Dispersion Technology Inc., 364 Adams Street, Bedford Hills, NY 10507, USA*

Received 23 April 2004; accepted 22 October 2004

## Abstract

Water-in-kerosene emulsion stabilized with SPAN surfactant exhibits a slow transition (on scale of hours) from an emulsion to a mini-emulsion state. We continuously monitor this transition in the relatively concentrated samples (5 vol.% water), without dilution, using acoustic, electroacoustic and conductivity measurements. Continuous stirring prevents sedimentation. We confirm our measurements with microscopic image analysis and by comparing with a stable water-in-car oil microemulsion stabilized with AOT.

Acoustic measurements yield information about the droplet size evolution in time. The original droplets, having a size of about 0.4  $\mu\text{m}$ , slowly coalesce into larger droplets. After 10 h the droplet size has increased to about 5  $\mu\text{m}$ . At this point a mini-emulsion fraction appears with a droplet size of only 25 nm and the droplet size distribution becomes bimodal. It takes another 24 h for the emulsion droplets to completely transform into a mini-emulsion state.

The conductivity exhibits a rapid change during the first 10 h of emulsion coalescence, but the rate becomes much slower as the mini-emulsion fraction begins to grow.

Electroacoustic measurements shows that the original emulsion droplets carry a substantial surface charge, which we are able to calculate using Shilov's theory for overlapped DLs.

The measured electroacoustic signal gradually decays with time. In the final state the mini-emulsion droplets generate practically no electroacoustic signal and appear uncharged. This fact, combined with conductivity measurements, indicates a strong role for electrostatic factors in emulsion stability and its transition to mini-emulsion state. We suggest that ion exchange between the exterior and interior diffuse layers leads to a gradual collapse of the exterior DL and explains all the experimental observations.

© 2004 Elsevier B.V. All rights reserved.

**Keywords:** Water-in-oil emulsion; Mini-emulsion droplets; Experimental observations

## 1. Introduction

It is known that heterogeneous liquid-in-liquid system can exist in two general states:

- thermodynamically unstable emulsion with a droplet size range on scale of microns;
- thermodynamically stable microemulsion with a droplet size range on scale of nanometers.

Depending on the properties of the liquids, the surfactant content, the temperature, and mixing conditions, either of these states might initially emerge. For instance, according to the classic review by Davies and Rideal [1], there are at least three possible mechanisms for spontaneous emulsification that might occur when two immiscible liquids are placed in contact with each other, even without stirring. These mechanisms are: (1) interfacial turbulence; (2) negative interfacial tension; (3) diffusion and stranding. Various authors have recently proposed additional mechanisms as described in the review [2]. All of these papers relate to emulsions, but it is also clear that if thermodynamic conditions allow, microemulsions might also form spontaneously right after mixing.

\* Corresponding author.

E-mail address: adukhin@dispersion.com (A. Dukhin).

It is also known that under certain conditions emulsions can be converted into microemulsions, and vice versa. For instance, review [2] mentions several reports in which simply a quick shift in temperature induced a microemulsion–emulsion transition, paper [3] as an example. There is also an extensive theoretical review in [2] of various models describing spontaneous emulsification.

An emulsion–microemulsion transition is defined by a large change in droplet size. The size of emulsion droplets is normally measured on a micron scale, whereas the size of the microemulsion droplets is in the nanometer range. However, this difference in sizes is not an absolute rule. There are more and more instances reported in literature of emulsions with rather small droplet size. There is a special term introduced for these systems—mini-emulsions. They can be identical to microemulsions in droplet size, but still thermodynamically non-equilibrated as typical emulsions.

In this paper we describe our observations on how a water-in-oil emulsion evolves into a mini-emulsion. We are able to monitor this slow transformation thanks to new Acoustic and electroacoustic characterization techniques based on ultrasound [4]. These methods eliminate the need for any sample preparation or dilution and allow us to continuously characterize the emulsion evolution in time.

Acoustic spectroscopy yields information about the particle size distribution. This method has several advantages over light scattering and other sizing techniques that turn out to be crucial for this work. For instance, this method is much more suitable for polydisperse systems than light scattering because weight basis is the innate basis of the measurement, as with sedimentation. This is the only way to monitor droplets with sizes on micron and nanometer scale simultaneously.

Acoustic measurements are particularly useful if they can provide data over a wide frequency range, for example 1–100 MHz. Emulsion droplets contribute to acoustic attenuation at low frequencies below 10 MHz, whereas microemulsion droplets affect primarily the high frequencies around 100 MHz. This investigation shows that only those ultrasound-based instruments that are able to cover this wide frequency range are suitable for characterization of emulsions and mini/microemulsions.

The other ultrasound-based technique, electroacoustics, offers unique opportunities for characterizing electric surface properties of emulsions and mini–microemulsions. Although traditional microelectrophoretic experiments [5,6] do reveal the importance of the electric surface charge on the water–oil interface, they are restricted to working with very dilute systems. There is always ambiguity left regarding the effect of the dilution on the emulsion.

Electroacoustics do not require dilution. This allows us to monitor the variation of electric surface properties continuously over many hours.

Electroacoustics offer one more advantage over more traditional methods. It is able to give information about the electric surface properties in non-polar liquids, whereas mi-

croelectrophoresis, with regard to emulsions, is restricted to aqueous systems. The most extensive evaluation of the water–oil interface charging has been made using oil-in-water emulsions [6]. The most recent review of the emulsion electrokinetics [5] mentions only aqueous emulsions.

Electroacoustics in non-polar liquids employs a new theory, recently created by Shilov et al. [7]. This electroacoustic theory takes into account overlap of DLs and other peculiar features of non-polar systems [8–10]. We present some predictions of this new electroacoustic theory with regard to the water-in-oil emulsions in Appendix A.

In this work we deal only with water-in-oil emulsions. Electroacoustics gives us the means to correlate the variation in the electric surface properties with variation of the droplet size. This is very important information for determining the role of electrostatic factors in emulsion stability.

Summarizing, we can formulate the following two goals of this paper:

- studying water-in-oil emulsions and mini–microemulsions;
- illustrating new methods for characterizing emulsions and mini–microemulsions.

In order to achieve these goals we use our experience with the SPAN family of surfactants in kerosene. In our previous papers we showed that the conductivity linearly correlates with the concentration of SPAN [15]. This gives a simple way to control the ionic composition of a non-polar liquid. Water-in-kerosene emulsions with SPAN surfactants are very simple and reproducible in preparation. They exhibit very interesting evolution in time, starting with coalescence and then 10 h later beginning a transformation into a mini-emulsion.

## 2. Materials and methods

We used the surfactant sorbitan mono-oleate, known also as SPAN 80, by Fluka. We used three different surfactant contents 0.5, 1 and 5 wt.% relative to kerosene. System with 1% is the most convenient for illustrating observed effects.

We used kerosene from the hardware store. We tried several producers of kerosene and discovered practically no influence of the kerosene origin on the results of measurements. We used a value of 2 for the dielectric constant of kerosene because it is not clear how impurities would affect this number.

We used distilled water and water with 0.01 M KCl.

For emulsion preparation we add water to the kerosene solution with a certain concentration of the SPAN. Then we sonicate this solution for 2 min. The water content is 5 vol.% in all samples.

We measured the droplet size of water in the kerosene emulsions using the DT-1200 by dispersion technology. The acoustic sensor of this instrument allows us to characterize the particle size without dilution (for detail description see [4]). The average measurement time for these samples is about

6 min. These emulsions require continuous mixing to prevent settling, which is provided by the built-in magnetic stir bar in the DT-1200 sample chamber.

Kerosene evaporates if chamber remains open. Prevention of this effect is not trivial in the case of acoustic measurement because variable gap between transducer and receiver causes variation of the internal chamber volume over the time. In order to minimize this effect we cover top of the chamber with flexible latex glove that could expand and contract during the measurement.

For conductivity measurements we used a Model 627 Conductivity Meter by Scientifica. It operates at 18 Hz with an applied voltage of about 5 V<sub>rms</sub>. The measurement range is from 20 to 20,000 pS/cm.

For electroacoustic measurement we use the Zeta Potential Probe DT-300 (for detailed description see [4]). This probe could be inserted directly into the sample vessel, as it is shown in Fig. 1. An external magnetic mixer prevents settling of particles.

Prevention of kerosene evaporation during conductivity–electroacoustic measurement is more complicated because of the conductivity probe structure. This probe consists of the two co-centric cylinders. Flow of liquid should move through the probe. We insert this probe into the DT-1200 chamber from the top. Connecting cable creates problem for airtight sealing. In addition kerosene vapor affects properties of the sealant. As a result we are able to keep chamber sealed for re-

stricted amount of time, shorter than in the case of the acoustic measurement.

We tested reproducibility of the observed effect by repeating the same experiment several times. All together we have made 4313 measurements during 4 months from December 2003 to April 2004. We present some of these repeated runs below.

### 3. Droplet size evolution by acoustic measurement

The attenuation frequency spectrum is the raw data for calculating the droplet size distribution. Fig. 2 shows the attenuation curve as it evolves in time. Fig. 3 illustrates just trends using simpler two-dimensional presentation. It indicates that low frequency attenuation begins to decay right after sonication stops. The high frequency attenuation begins to increase with a 10 h delay.

Increase of the high frequency attenuation is the most striking feature of this process. It is quite reproducible as shown in Fig. 4. It occurs at different water and surfactant contents.

This evolution of the attenuation spectra reflects the variation of the droplet size distribution. The procedure and theory for the calculation the droplet size distribution from these attenuation spectra is given in our book [4].

Fig. 5 presents the droplet size distribution calculated at 5 h intervals. Table 1 presents input parameters that are required for performing this calculation.

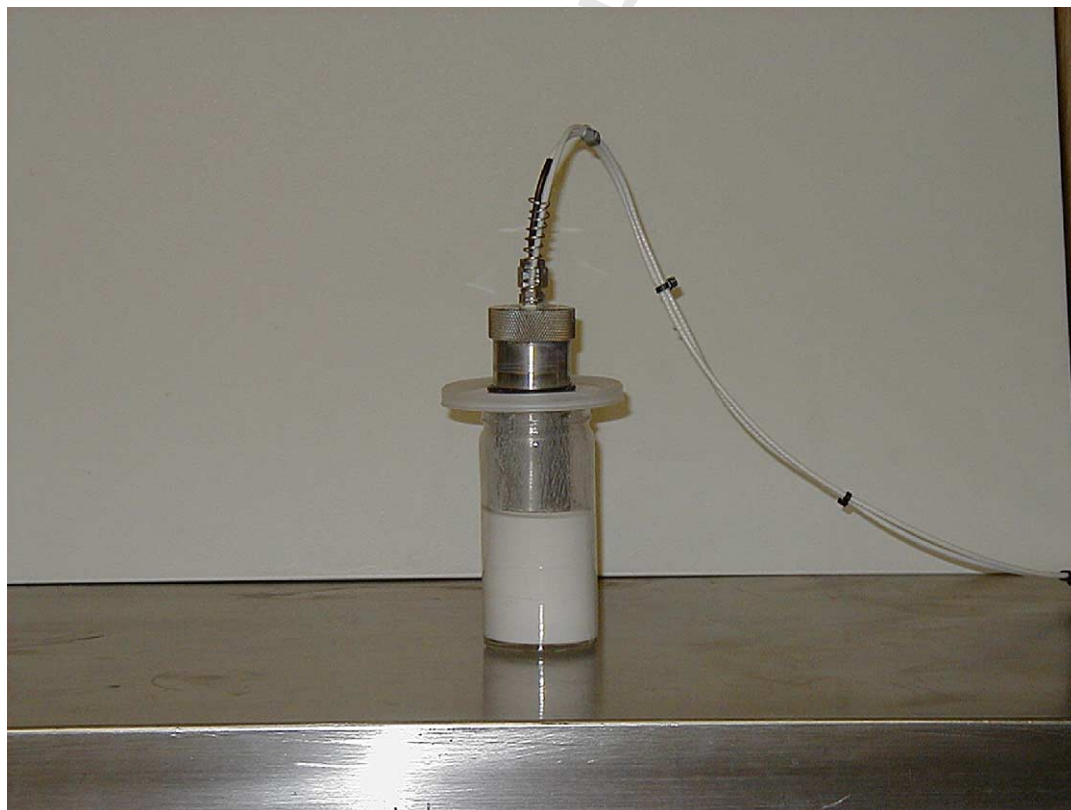


Fig. 1. Photograph of DT-300 Zeta Potential Probe inserted into the alumina–kerosene–SPAN 80 dispersion.

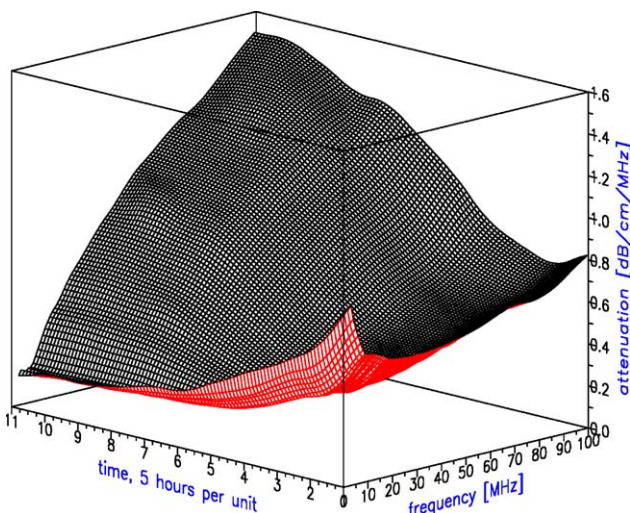


Fig. 2. Attenuation frequency spectra evolution in time.

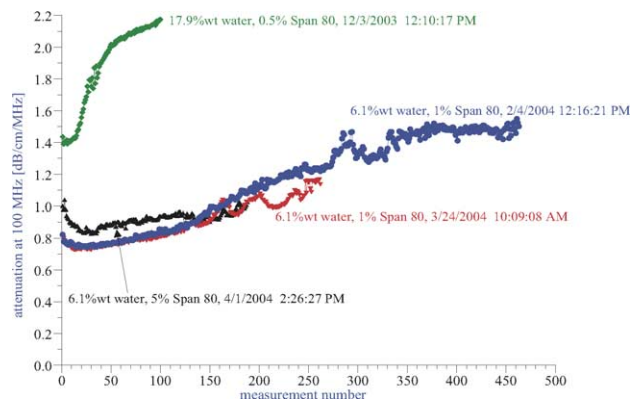


Fig. 4. Evolution of the attenuation at 100 MHz in time for various emulsions. Reproducibility test with 6.1 wt.% water-in-kerosene emulsion with 1 wt.% of SPAN 80.

181 It is seen that during the first 10 h the droplet size mono-  
 182 tonically increases, corresponding to simple coalescence of  
 183 the original emulsion droplets. During this initial period the  
 184 median droplet size changes roughly from 0.4 to 2  $\mu\text{m}$ .

185 Then, suddenly after 10 h a fraction with an average size of  
 186 25 nm appears. The content of this fraction increases during  
 187 the next 30 h. The emulsion fraction continues to coalescence  
 188 during this time, eventually reaching a size of about 7  $\mu\text{m}$ .

189 The third period in the emulsion evolution begins roughly  
 190 after 40 h. At this point the emulsion converts completely to  
 191 the small size state. After this the attenuation spectra becomes  
 192 stable and evolution of the droplet size stops.

193 Comparison of these droplet size distributions with atten-  
 194 uation spectra reveals a very simple correlation. The atten-  
 195 uation at low frequencies below 10 MHz corresponds to the

196 emulsion droplets, whereas the small size droplets contribute  
 197 to the high frequency attenuation.

198 Droplet size distributions in Fig. 5 are result of automatic  
 199 calculation performed by DT-1200 software. It interprets atten-  
 200 uation as a combination of intrinsic losses and thermal  
 201 losses. Intrinsic losses are independent on the droplet size.  
 202 It is simple volume averaged ultrasound attenuation in ho-  
 203 mogeneous materials of the dispersed phase and dispersion  
 204 medium. Thermal losses are droplet size sensitive, according  
 205 to the theory presented in our book [4].

206 Fig. 6 presents contribution of these two attenuation mech-  
 207 anisms to the last attenuation from the set presented in Fig. 2.  
 208 It is seen that theoretical attenuation fits experiment pretty  
 209 well with a fitting error of 5.6%. This fitting corresponds to

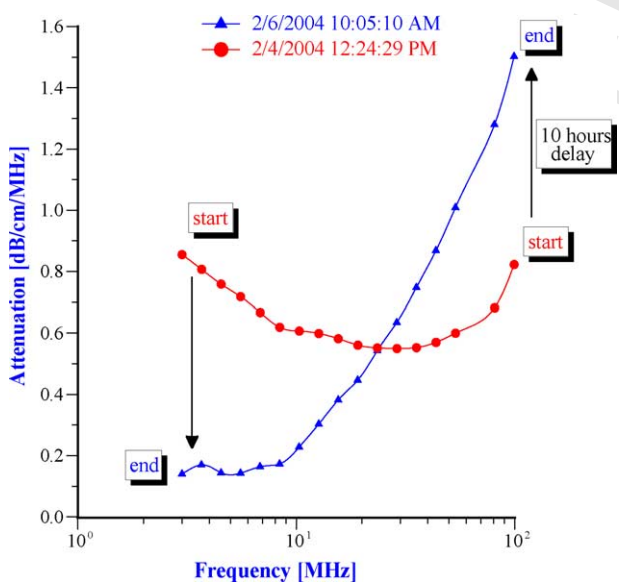


Fig. 3. Attenuation frequency spectra at the beginning and at the end of the experiment. Arrows show trends in attenuation evolution.

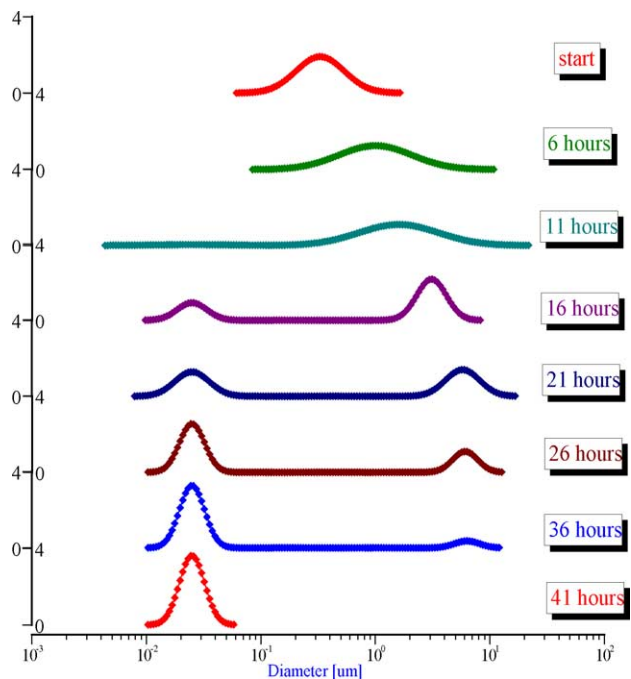


Fig. 5. Evolution of the droplet size distribution in time.

Table 1  
Thermodynamic properties of the kerosene and water phases around room temperature

	Density (g/cm <sup>3</sup> )	Thermal conductivity (J/ms K)	Heat capacity (J/kg K)	Thermal expansion (10 <sup>-4</sup> K <sup>-1</sup> )	Attenuation (dB/cm/MHz) – frequency (MHz)
Water	0.997	0.61	4.18	2.07	$\alpha = 0.002\omega$
Kerosene	0.81	0.15	2.85	10.6	$\alpha = 0.0106\omega$

210 the lognormal droplet size distribution with the median size  
211 17 nm and standard deviation 0.22.

212 In principle, there is another possibility for high frequency  
213 attenuation interpretation. It might be related to the scattering  
214 losses, instead of the thermal losses. In this case calculation  
215 would yield a larger droplet size with increasing high frequency  
216 attenuation. It is important to clarify why DT-1200  
217 software ignored this option and selected thermal effect over  
218 scattering. We could answer this question by forcing searching  
219 routine in DT-1200 software into the particular range of  
220 large sizes above 5 μm.

221 The best solution in this range and corresponding theoretical  
222 fitting are shown in Fig. 7. The best median droplet size is  
223 11.7 μm. This droplet size distribution yields theoretical at-  
224 tenuation that fits experimental data with error of 21.6%. This  
225 error is much larger than in the case of the thermal attenuation  
226 assumption (5.6%). This is the reason why DT-1200 software  
227 selected small droplet size with corresponding thermal mech-  
228 anism over larger droplet sizes with scattering mechanism.

229 At the same time, combination of intrinsic and ther-  
230 mal attenuation for only small droplet does not provide a

231 perfect fit. It is our experience that fitting error of 5.6%  
232 is still quite large. We think that it happens because of  
233 the presence of small fraction of the large droplets. Pres-  
234 ence of this fraction could explain levelling of the attenu-  
235 ation curve at low frequency as it is shown in Fig. 3 for  
236 the curve marked “end”. Instead of becoming practical 0  
237 at low frequency it becomes stable at the level of about  
238 0.1 dB/cm/MHz when frequency is below 10 MHz. It is clear  
239 indication of the larger emulsion droplets. Unfortunately this  
240 attenuation is not sufficient to determine size and amount  
241 of this droplets. That is why DT-1200 software has sim-  
242 ply ignored them. Inability to fit perfectly this part of at-  
243 tenuation spectra determines relatively large fitting error of  
244 5.6%.

245 We would like to stress the importance of being able to  
246 collect attenuation data over a wide frequency range. The  
247 absence of frequency data below 20 MHz would simply miss  
248 the variation of the emulsion fraction. Similarly, the absence  
249 of high frequency data would miss the variation due to the  
250 small size fraction.

251 At this point in the discussion we do not know the nature  
252 of the small droplets. They might be either microemulsion

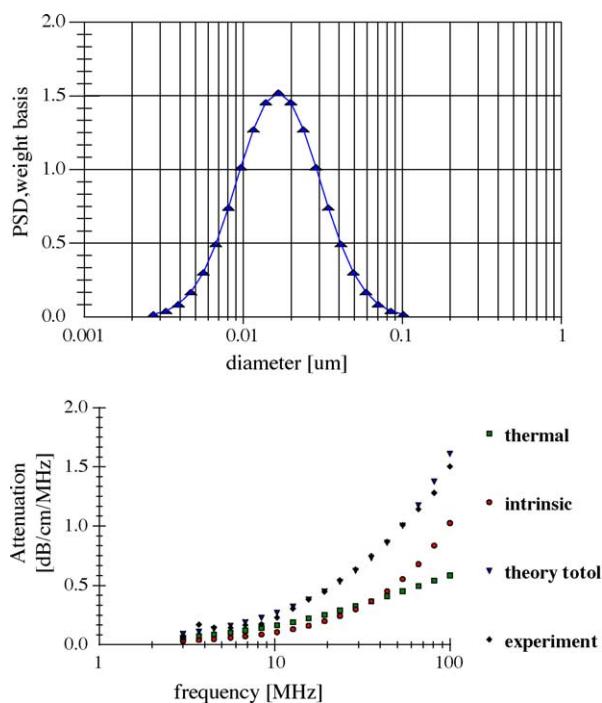


Fig. 6. Droplet size of the final mini-emulsion and corresponding experimental and theoretical attenuation spectra. Droplet size does not reflect small amount of large droplets because attenuation spectra does not contain enough information for its determination.

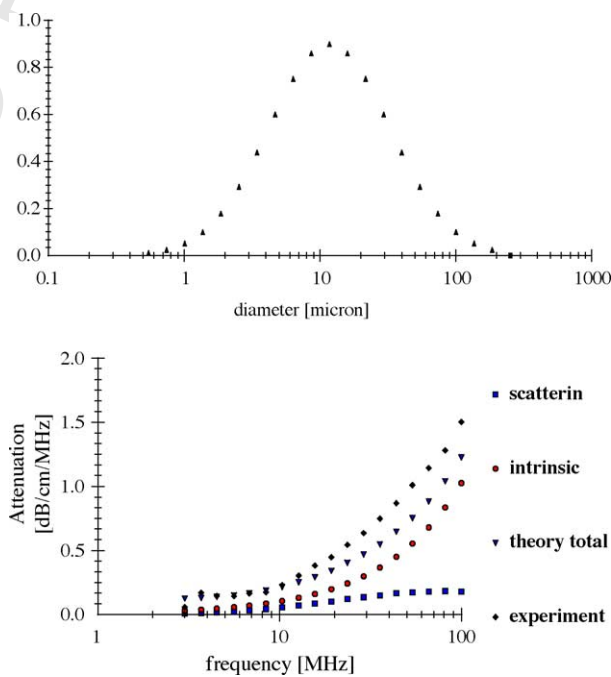


Fig. 7. The best droplet size distribution assuming scattering mechanism of ultrasound attenuation. Corresponding theoretical attenuation that fail to fit experimental data.

253 or mini-emulsion droplets. We use sedimentation analysis  
 254 and image analysis to answer this question. We also do not  
 255 know at this point the reason for the strange kinetic behavior.  
 256 Next we will consider electroacoustic measurements to help  
 257 get these answers, because it yields information about the  
 258 surface properties of the water droplets.

#### 259 4. Mini-emulsion or microemulsion?

260 The evolution of the emulsion described in the previous  
 261 section occurs under conditions of continuous stirring. We  
 262 use a magnetic stirrer to prevent sedimentation of the original  
 263 emulsion.

264 If we turn the stirrer off after the system reaches a steady  
 265 state, the water droplets sediment. If system was a thermody-  
 266 namically microemulsion, we would observe no sedimenta-  
 267 tion effect. Hence sedimentation points toward a thermody-  
 268 namically unstable mini-emulsion. This mini-emulsion turns  
 269 into sedimenting emulsion when stirrer is turned off.

270 At the same time there is no phase separation. If we turn  
 271 the stirrer on again, the system exhibits the same acoustic  
 272 properties as before sedimentation occurred with the same  
 273 small droplet size.

274 These observations indicate that we are dealing with an  
 275 unstable mini-emulsion, which undergoes coalescence after  
 276 stirring is turned off.

277 We performed two tests for confirming this conclusion.

278 First of all we compared acoustic properties of this un-  
 279 stable system with acoustic properties of another water-in-  
 280 oil emulsion, which becomes definitely microemulsion after  
 281 adding surfactant. It is water-in-car oil with AOT as stabilizer.  
 282 Water in pure car oil builds up emulsion under influence of  
 283 sonication, even without any additional surfactant. We pre-  
 284 pared such emulsion at 5 vol.% applying 1 min of sonication.  
 285 Final emulsion has a white color, which is specific for emul-  
 286 sions. It indicates very high turbidity associated usually with  
 287 droplet sizes on micron scale.

288 Attenuation spectra and corresponding droplet size for this  
 289 emulsion are shown in Fig. 8. Median size is about 2  $\mu\text{m}$ , as  
 290 expected.

291 At the second stage of this experiment we added 1% of  
 292 AOT to this emulsion. After 1 min of sonication this liquid  
 293 becomes transparent with color practically identical to the  
 294 color of the original car oil. This simple observation is a def-  
 295 inite proof that AOT converts emulsion into microemulsion.  
 296 Fig. 8 shows that acoustic properties have changed dramati-  
 297 cally as well. Attenuation becomes much smaller. Median  
 298 droplet size becomes about 10 nm.

299 This experiment shows that there is clear correlation  
 300 between acoustics and optical properties of the stable  
 301 emulsion–microemulsion transition.

302 We could now compare attenuation spectra of water-in-  
 303 kerosene emulsion (Fig. 3) with water-in-car oil emulsion  
 304 (Fig. 8). There is clear similarity between these curves.  
 305 We know that low attenuation curve in the case of water-

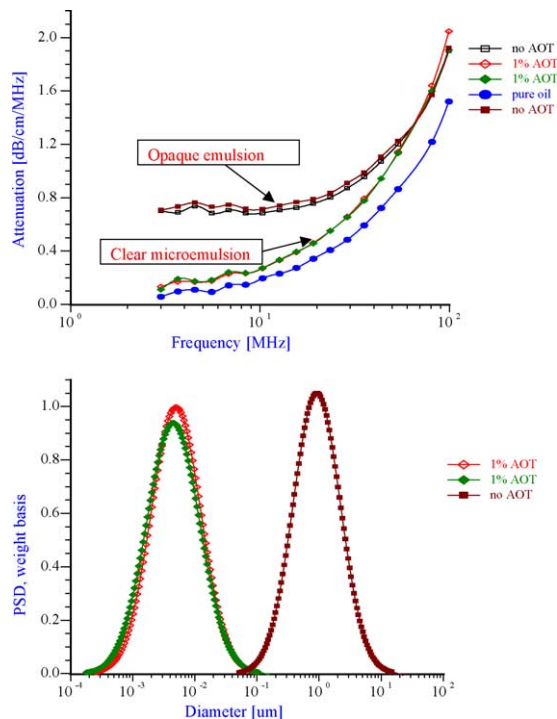


Fig. 8. Attenuation spectra of 5 vol.% water-in-car oil emulsion and microemulsion stabilized with 1% AOT. Corresponding droplet size distributions.

in-car oil corresponds to the stable and optically transparent  
 microemulsion. This could be used as justification of  
 our earlier conclusion that lower attenuation at low fre-  
 quency is indication of the smaller droplets sizes in the  
 case of water-in-kerosene emulsion at the final stages of its  
 evolution.

Unfortunately optical test in the case of the water-in-  
 kerosene emulsion is not that definite as in the case of the  
 water-in-car oil emulsion. Water-in-kerosene emulsion re-  
 mains opaque independently on variation of the acoustic  
 properties. However, it is not sufficient to claim that there  
 is no small mini- or microemulsion droplets in the system  
 at the end of its evolution. Small amount of larger droplets  
 could be responsible for the high turbidity.

In order to verify this hypothesis we performed a micro-  
 scopic analysis of the final system after 40 h of stirring. We  
 used a dark field microscope with a digital camera to capture  
 images continuously for an hour.

Fig. 9 shows five snapshots of the emulsion image at inter-  
 vals of 10 min. It is clearly seen that the size of the emulsion  
 droplets grows with time. However, the large droplets of mi-  
 cron size do not coalesce. The growth that we observe is  
 apparently related to the capturing of the very small droplets  
 by the larger ones. These small droplets look like bright dots  
 in the dark field. Microscopy does not allow estimate of their  
 sizes, which are clearly less than a micron.

This microscopic test confirmed that the system contains  
 a number of very small droplets, which slowly coalesce in  
 larger droplets with higher degree of aggregative sta-

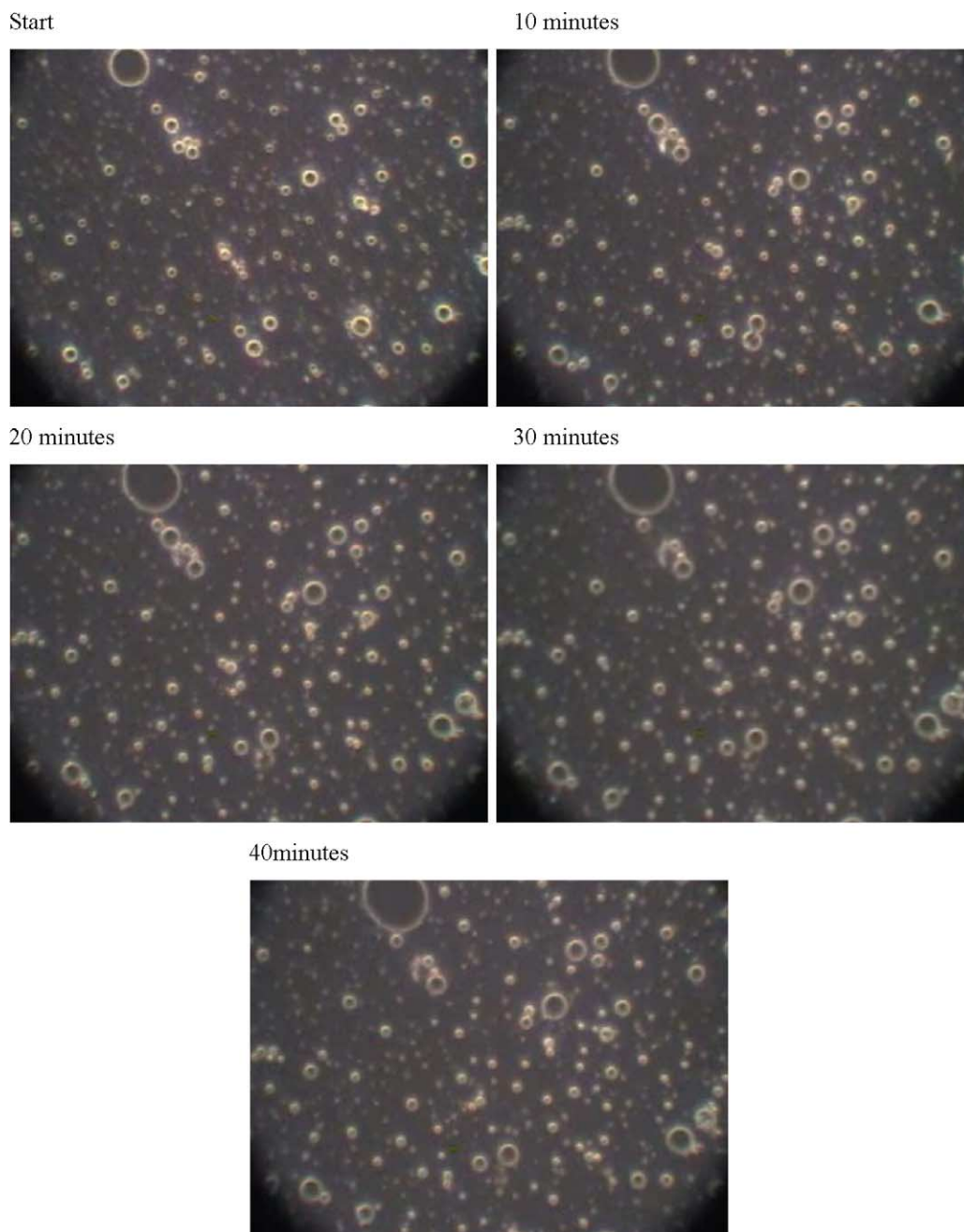


Fig. 9. Emulsion evolution after stirrer is turned off. The width of each picture is approximately 100  $\mu\text{m}$ .

335 bility. Stirring breaks quickly these large droplets into the  
 336 smaller ones. These small mini-emulsion droplets dominate  
 337 the acoustic attenuation, which is measured under stirring  
 338 conditions.

339 At the same time it confirms presence of larger droplets  
 340 with sizes on micron scale. This is the fraction that con-  
 341 tributes 0.1 dB/cm/MHz to the low frequency attenuation in  
 342 Fig. 3, curve “end”. Apparently volume fraction of these  
 343 large droplets is not sufficient for being reflected in the  
 344 droplet size distributions calculated from the attenuation  
 spectra.

345 Presence of this small fraction of larger droplets could ex-  
 346 plain high turbidity of the final mini-emulsion. Unfortunately  
 347 we could not estimate amount of these larger droplets neither  
 348 from acoustics nor from optical images.

## 5. Surface charge evolution by electroacoustic and conductivity measurements

351 Electroacoustic measurement in non-aqueous systems in-  
 352 volves three steps.

The first step is calibration with 10% silica Ludox in 0.01 M KCl aqueous solution. The  $\zeta$ -potential of this dispersion is  $-38$  mV, which is the basis for calibration.

The second step is the measurement of the electroacoustic signal of pure kerosene. This gives us the value of the background or ion vibration signal. Presence of surfactant does not affect this background signal, as it is shown with measuring kerosene that contains the surfactant. The DT-1200 software allows us to save this value and to subsequently subtract this background signal from further measurements. It is vector subtraction because electroacoustic signal is a vector with a certain magnitude and phase.

As a simple test that this subtraction works, we measured kerosene again, this time making the background subtraction. This test gives us the value of the noise level of the electroacoustic measurement.

The third step is the actual measurement of the electroacoustic signal generated by the water-in-kerosene emulsion. This signal substantially exceeded the noise level, as shown in Figs. 10 and 11. Fig. 11 illustrates reproducibility of this effect.

With time, the CVI magnitude gradually decreases. Unfortunately we are not able to measure CVI continuously during 40 h with existing experimental setup. We mentioned before that measuring chamber must be airtight for preventing kerosene evaporation. Cable of the conductivity probe makes this hard to achieve. Simple sealant that we use becomes affected by kerosene vapor. That is why conductivity and CVI measurement are conducted only during 20 h, as it is shown in Figs. 10 and 11.

However, we are able to measure conductivity and CVI of the final emulsions as a single point measurement even days after experiment finished. For instance, we stored emulsion after 40 h of the attenuation measurement. Later we could use this emulsion for CVI and conductivity measurement. For instance, after 8 days two consequent measurements CVI

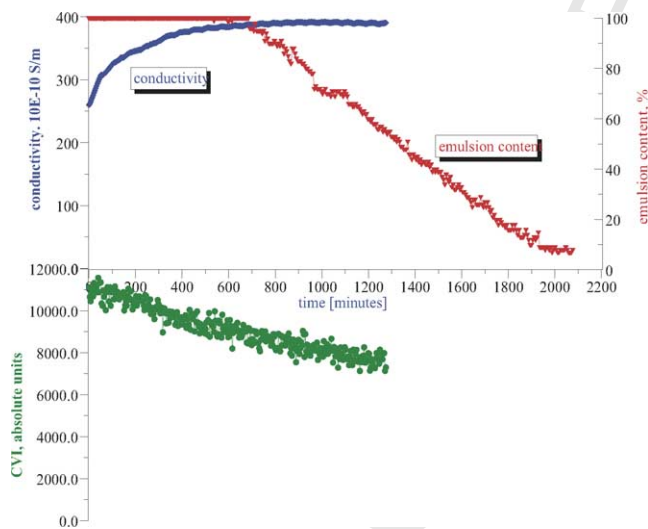


Fig. 10. Correlation between emulsion droplets content and measured conductivity and electroacoustic signal.

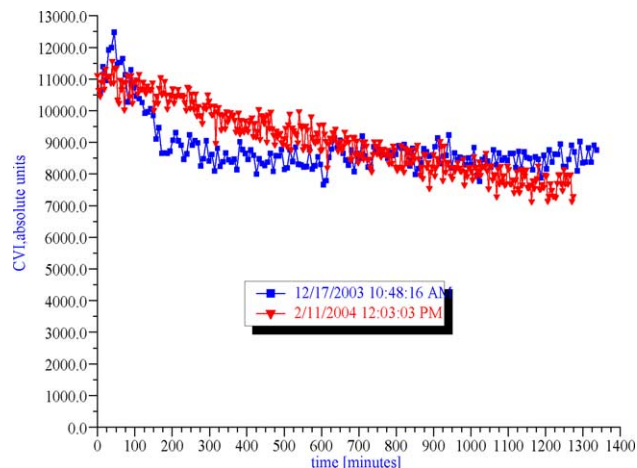


Fig. 11. Illustration of reproducibility of the effect and electroacoustic measurement.

yields values 1318 and 1973. That is why we could state that eventually CVI reaches the noise level.

From this CVI behavior with time we can conclude that:

- the microemulsion droplets do not contribute to the CVI signal;
- the emulsion droplets do contribute to the CVI signal.

There are several ways to explain the peculiarities of this system, which will be discussed below.

We can use the CVI values at the initial stage of coalescence for calculating the surface charge  $\sigma$  of the water droplets. According to Shilov's theory (Appendix A, Eq. (A.8)), this calculation requires certain input parameters, such as the properties of liquids and the size of the water droplets. Acoustic attenuation measurements yield information about the droplet size. As for the liquids properties, we use the following values:  $\rho_m = 0.8$  g/cm<sup>3</sup>;  $\rho_p = 1$  g/cm<sup>3</sup>;  $\eta = 1.5$  cp;  $\varepsilon_m = 2$ ;  $\varepsilon_p = 80$ . All these parameters are corrected for temperature.

Fig. 12 shows the resulting values for the surface charge evolution during the stage of emulsion coalescence. It is seen that it decays quickly with time, decreasing by almost 10 times during first 10 h. Surface charge decays with time much faster than CVI (Fig. 11) because droplet size increases almost five times during this period. Eq. (A.8) indicates that dynamic mobility and accordingly CVI are proportional to the product of the surface charge by the droplet size.

The question arises about the mechanism for this effect. Does this mean that the adsorbed SPAN molecules are losing charges they carry to the surface? Is there any other explanation that would not involve restructuring of the SPAN molecules?

In answering these questions we should keep in mind a clear correlation between the apparent surface charge decay and the conductivity increase, as shown in Fig. 10. It appears that the droplets release ions into the kerosene while coalescing. We suggest a model that explains this feature in the next section.

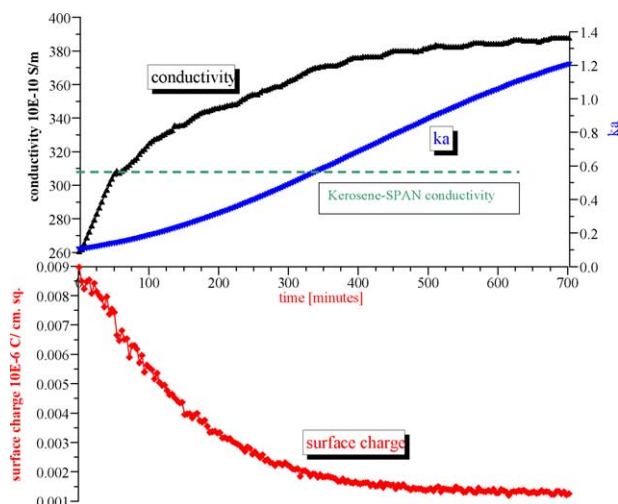


Fig. 12. Correlation between measured conductivity and calculated apparent surface charge density.

It is important to mention that the conductivity of the initial kerosene–SPAN 80 solution is about  $310 \times 10^{-10}$  S/m. The conductivity of the initial emulsion is less than this value. It appears that the water droplets adsorb SPAN and reduce the conductivity. However, with time the conductivity increases, eventually exceeding the initial value in the kerosene–SPAN solution (see Fig. 10).

Conductivity measurements allow us to estimate the  $\kappa_a$  value and determine the validity of Shilov's theory in regard to this system. It is known that Shilov's theory is valid only for overlapped DLs. Fig. 13 shows the relationship between the volume fraction and  $\kappa_a$  for overlapped DLs. A more detailed description is given in our book [4]. It is seen that at a volume fraction of 5% the DLs do overlap if  $\kappa_a < 1$ . This is the range of  $\kappa_a$  values when Shilov's theory can be applied.

Fig. 12 presents  $\kappa_a$  values calculated using the measured conductivity and the particle size computed using attenuation spectroscopy. We also assumed that there are simple small

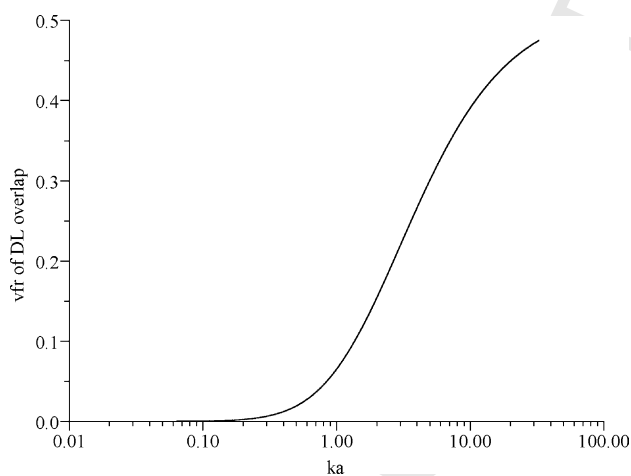


Fig. 13. Estimate of the volume fraction of the overlap of the electric double layer.

ions in the kerosene phase with an approximate diffusion coefficient of  $10^{-5}$  cm<sup>2</sup>/s. If this assumption is valid,  $\kappa_a$  satisfies the condition of overlapped DLs during the complete initial period of emulsion coalescence. This is a justification for using Shilov's theory for calculating the surface charge.

In the next section we suggest a model that links together these experimental data.

## 6. Discussion

We have established that the evolution of the water-in-kerosene emulsion with SPAN 80 as emulsifier proceeds in three distinct periods.

*Period 1: first 10 h.* The water droplets are coalescing. The apparent surface charge of the droplets decays. The conductivity increases, eventually exceeding the initial value in the kerosene–SPAN solution.

*Period 2: between 10 and 40 h.* The mini-emulsion fraction appears and grows. The emulsion droplets continue to coalescence. The CVI continues to decay. The rate of conductivity increase is much smaller.

*Period 3: after 40 h.* All parameters are stable. There are no emulsion droplets. The water is in mini- and possibly microemulsion droplets. These droplets do not generate any CVI signal.

It is quite possible that there are multiple explanations of this set of facts. Here we just suggest one of them. We do not claim that it is the only one. We want to be absolutely clear that it is just one of, perhaps, several possible models.

Our model is based on the assumption that the water–kerosene interface with adsorbed SPAN remains unchanged. We assume that the SPAN molecules stabilized this interface almost instantly during initial sonication and brought it to thermodynamic equilibrium. However, it is only a local equilibrium for each small element of the interface.

The part of the SPAN molecules in the bulk of the solution is responsible for the conductivity of the original kerosene–SPAN solution. It means that they carry charge, either as individual molecules, or as micelles (see our previous paper [15]).

It is also possible that at least a fraction of the adsorbed SPAN molecules is charged and brings this charge to the surface.

We assume that the electric charge of the water–kerosene interface that is associated with adsorbed SPAN molecules remains constant, time independent. Local thermodynamic equilibrium is the justification for this assumption.

We attribute the observed evolution of the parameters to ion exchange between the interior of the water droplets and the bulk of the kerosene solution.

Initially the water droplets have an electro-neutral interior. Ions are trapped inside of the large water droplet at about equal amounts. The surface charge induced by adsorbed SPAN molecules is screened with an external diffuse layer in the kerosene solution. Fig. 14 illustrates this structure.

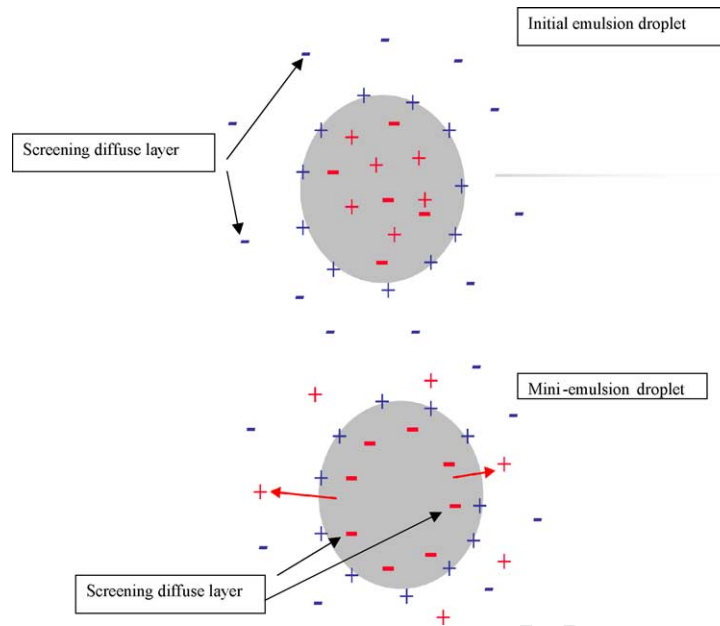


Fig. 14. Illustration of the double layer restructuring due to the ion exchange between interior and exterior of the water droplet.

497 The external diffuse layers are very thick due to the low  
 498 ionic strength. They are overlapped. This gives rise to the  
 499 CVI signal. We could estimate the amount of energy  $W_{ext}$   
 500 required to charge this external DL to a certain level of  
 501 surface charge  $Q$  as:

$$502 \quad W_{ext} = \frac{Q^2}{2C_{ext}} = \frac{Q^2}{\epsilon_p \epsilon_0 S \kappa_{ext}} \quad (1)$$

503 where  $S$  is the surface area,  $\kappa_{ext}$  the Debye parameter for  
 504 external DLs.

505 Obviously, there is another possibility to screen the sur-  
 506 face charge induced by SPAN adsorption. It could be done  
 507 with screening diffuse layer inside of the particle. This sec-  
 508 ond opportunity would also take a certain amount of energy,  
 509 which we could estimate with following equation:

$$510 \quad W_{in} = \frac{Q^2}{2C_{in}} = \frac{Q^2}{\epsilon_p \epsilon_0 S \kappa_{in}} \quad (2)$$

511 Comparison of these two charging energies yields the fol-  
 512 lowing approximate result:

$$513 \quad \frac{W_{in}}{W_{ext}} = \frac{\epsilon_m \kappa_{ext}}{\epsilon_p \kappa_{in}} = \sqrt{\frac{\epsilon_m K_m}{\epsilon_p K_m}} = \sqrt{\frac{K_m}{40 K_p}} \approx 0.001 \quad (3)$$

514 where we have assumed that the conductivity of water is about  
 515  $10^6/40$  times larger then conductivity of kerosene, the effec-  
 516 tive diffusion coefficients  $D_{eff}$  being the same, and that the  
 517 Debye parameter can be given with the following equation:

$$518 \quad \kappa^2 \approx \frac{K}{\epsilon_0 \epsilon D_{eff}} \quad (4)$$

519 This is certainly a very approximate estimate. However, it  
 520 clearly indicates that charging of the interior DL to a certain

electric charge is orders of magnitude more energy efficient  
 than exterior one.

It is important to mention that charging up to a certain  
 level of the electric potential, instead of the electric charge,  
 would lead to the opposite conclusion. We believe that in this  
 case we are dealing with the constant surface charge case  
 because it is related to the adsorption of thermodynamically  
 determined amount of the surfactant.

The above-mentioned difference in energy for charging  
 the DLs creates a driving force for co-ions to leave the in-  
 terior of the droplet. This simply means that there is a gradi-  
 ent of co-ions electrochemical potential that drives co-ions  
 from the droplet out. This statistical process is slow because  
 ion should become solvated by surfactant molecules on the  
 kerosene–water interface. It is known [10] that only suffi-  
 ciently large ions could exist in non-polar liquids. This slow  
 leakage of co-ions from the droplet generates an internal elec-  
 tric charge that would screen the adsorbed surface charge.  
 Eventually this would lead to the complete collapsing of the  
 external DL. The surface charge of the adsorbed SPAN  
 would be completely compensated by the interior charge of  
 the water droplet. Fig. 14 illustrates this final stage of the  
 transition.

This model could explain all observed features of the  
 emulsion–mini-emulsion transition.

First of all, it explains why the conductivity increases dur-  
 ing the coalescence period and eventually significantly ex-  
 ceeds the conductivity level of the original kerosene–SPAN  
 solution (see Fig. 10). This excess conductivity comes from  
 the counter-ions released from the water droplets into the  
 kerosene.

Alternative model that could potentially explain some of  
 the observed facts with restructuring of the adsorbed SPAN

molecules would not explain the excess conductivity. This is a serious argument supporting the “ion exchange model”.

The “ion exchange model” also explains the lack of the CVI signal for the microemulsion. It happens because the surface charge of the adsorbed SPAN molecules is completely screened with the internal charge of the microemulsion droplet. Consequently it looks from the outside as being electro-neutral.

In this model redistributing screening electric charge from the outside diffuse layer to the inside one is a limiting factor of the emulsion droplet break up into much smaller mini- and possibly microemulsion droplets. Apparently this break up occurs when a sufficient critical amount of energy is released due to the collapsing external DL.

Another potential factor controlling this break up, droplet size, seems not important at all. We could conclude this based on the observation that the size of the emulsion droplets continues to grow during period 2. If break up would relate to the droplet size, we would observe growth only up to certain maximum value of the size. It is obviously not the case.

This break up is not exactly a spontaneous one because it strongly depends on the presence of stirring. However, stirring with magnetic stir bar in the DT-1200 chamber is not a vigorous one. It is clear that reduction of the surface tension is a most important factor. In this sense the observed phenomena is similar to the “negative interfacial tension” mechanism of spontaneous emulsification [2].

It is also possible that combination of stirring and reduction of the surface tension intensifies “interfacial turbulence” described in the paper [16].

At the end, we would like to repeat that the suggested mechanism explains all the experimental facts, but we could not claim that it is the only one to do so. There might be some other explanations of the phenomena presented in this paper.

## 7. Conclusions

We have established that water-in-kerosene emulsion with SPAN 80 as emulsifier undergoes transition from emulsion to mini-emulsion when being slowly stirred. This transition takes approximately 40 h and proceeds in three distinct periods.

*Period 1: first 10 h.* Water droplets are coalescing. The apparent surface charge of the droplets decays. The conductivity increases, eventually exceeding the initial value in the kerosene–SPAN solution.

*Period 2: between 10 and 40 h.* A mini-emulsion fraction appears and grows in amount. The emulsion droplets continue to coalesce. The CVI continues to decay. The rate of conductivity increase is much smaller.

*Period 3: after 40 h.* All parameters are stable. There are no emulsion droplets. Water is in mini-emulsion and possible microemulsion droplets. These small droplets do not generate CVI signal.

We concluded that ion exchange between the interior of the water droplets and the bulk of kerosene solution could explain these experimental observations making no assumption about restructuring of the adsorbed SPAN molecules with time. This ion exchange leads to a gradual collapse of the exterior diffuse layer. The surface charge associated with the adsorbed SPAN molecules becomes screened with an interior diffuse layer. This process leads to the reduction of the surface tension and eventual break up of the emulsion droplet into much smaller mini- and possibly microemulsion droplets. The decay of the CVI signal and increasing conductivity are results of this ion exchange.

## Appendix A. Electroacoustic theory for water-in-oil emulsions and its verification

It is known that existing electroacoustic theories [4,11–14] for both ESA and CVI effects do not take into account overlapping of the double layers (DL). There is only one exception, the recently created Shilov’s theory [7].

Assumption of isolated, not-overlapped, double layers requires either a large droplet radius  $a$  or a sufficiently high ionic strength leading to a shorter Debye length  $\kappa^{-1}$ . Fig. 11 illustrates approximately the range of volume fractions  $\varphi$  where assumption of isolated DLs is valid for given  $\kappa_a$ , following our book [4].

If we assume that thin DLs do not overlap, we can use a widely accepted expression for the dynamic electrophoretic mobility  $\mu_d$  (Eq. (5.28) in [4]), that is:

$$\mu_d = \frac{2\varepsilon_0\varepsilon_m\zeta(\rho_p - \rho_s)\rho_m}{3\eta(\rho_p - \rho_m)\rho_s} G(s, \varphi)(1 + F(Du, \omega', \varphi)) \quad (\text{A.1})$$

where  $\varepsilon_0$  and  $\varepsilon_m$  are dielectric permittivities of the vacuum and liquid,  $\zeta$  the electrokinetic potential,  $\eta$  the dynamic viscosity,  $\rho_m$ ,  $\rho_p$  and  $\rho_s$  the densities of liquid, particle and dispersion,  $\omega' = \frac{\omega}{\omega_{MW}}$ ,  $\omega_{MW} = \frac{K_m}{\varepsilon_0\varepsilon_m}$ ,  $K_m$  the conductivity of the media,  $\omega$  the frequency of ultrasound and  $Du = \kappa^\sigma/K_m a$  the Dukhin number that reflects the contribution of the surface conductivity  $\kappa^\sigma$ .

Function  $G$  presents the contribution of hydrodynamic effects, whereas function  $F$  reflects electrodynamic aspects of the electroacoustic phenomena.

In order to apply this theory to water-in-oil emulsions we should simply introduce the conductivity of the particles in the expression for function  $F$ . A water-in-oil emulsion can be considered as conducting particles in a non-conducting media. In order to achieve this we should simply use more general expression for the Dukhin number:

$$Du = \frac{K_p}{K_m} + \frac{\kappa^\sigma}{K_m} \quad (\text{A.2})$$

where  $K_p$  is the conductivity of water droplets.

This modified Dukhin number can be used in the general expression for the  $F$  function.

$$F(Du, \omega', \varphi) = \frac{(1 - 2Du)(1 - \varphi) + j\omega'(1 - \varepsilon_p/\varepsilon_m)(1 - \varphi)}{2(1 + Du + \varphi(0.5 - Du)) + j\omega'(2 + (\varepsilon_p/\varepsilon_m) + \varphi(1 - \varepsilon_p/\varepsilon_m))} \quad (A.3)$$

The properties of the water-in-oil emulsion allow us to approximate the value of this function. It is known that the conductivity of water is much higher than the conductivity of non-polar liquids. This means that

$$Du \approx \frac{K_p}{K_m} \gg 1 \quad (A.4)$$

In addition, the dielectric permittivity of water is about 40 times higher than the permittivity of non-polar liquids:

$$\frac{\varepsilon_p}{\varepsilon_m} \gg 1 \quad (A.5)$$

Using these two strong inequalities we can neglect 1 in comparison to the relevant parameters in Eq. (A.3). As a result we get the following approximate value for the function  $F$  in

water-in-oil emulsions:

$$F(Du, \omega', \varphi) \approx \frac{1 - \varphi - 2Du - j\omega'(\varepsilon_p/\varepsilon_m)}{1 - \varphi - 2Du + j\omega'(\varepsilon_p/\varepsilon_m)} = -1 \quad (A.6)$$

This approximate value is actually quite accurate due to the large conductivity and permittivity of water.

If we use this value for function  $F$  in Eq. (A.1) for the dynamic mobility, we would come to the interesting result:

$$\mu_d \left( \frac{K_p}{K_m} \gg 1, \frac{\varepsilon_p}{\varepsilon_m} \gg 1 \right) = 0 \quad \text{for thin isolated DLs only} \quad (A.7)$$

This means simply that *water-in-oil emulsions with isolated and thin DLs should not exhibit any electroacoustic effect.*

It is possible to give a simple explanation to this unexpected conclusion. In order to do this we compare the electric field structure induced by the relative particle-liquid motion for non-conducting and conducting particles, as illustrated in Fig. 15.

It is known that ultrasound generates particle motion relative to the liquid due to the density contrast. In drawing

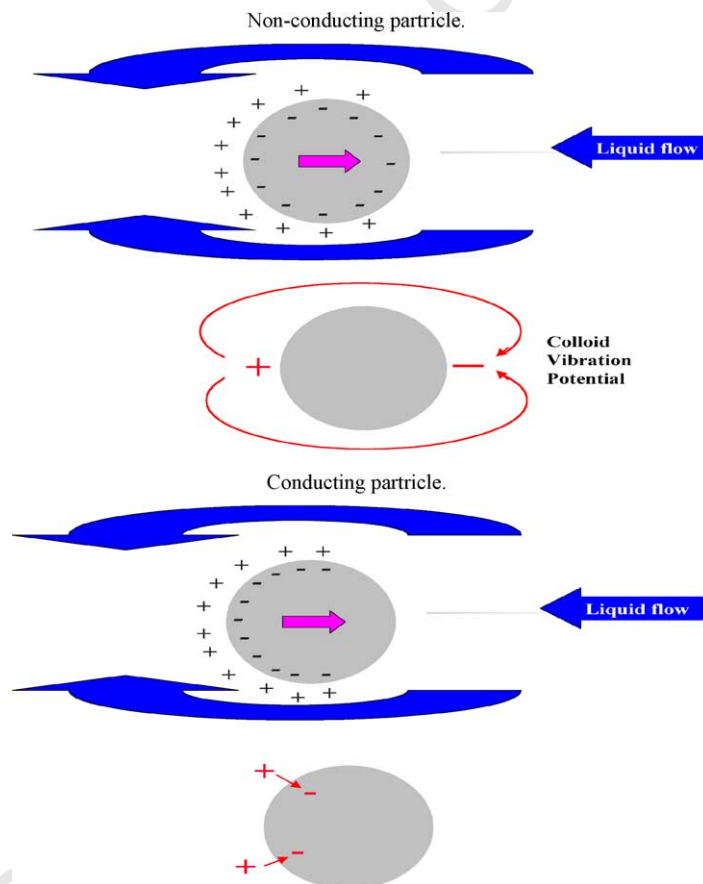


Fig. 15. Illustration of the exterior DL polarization by the liquid flow relative to the particle surface induced with ultrasound.

Fig. 15 we assume that the particles move from left to right. This causes a liquid motion, relative to the particle surface, which is illustrated with arrows above and below the particle.

This motion of the liquid drags ions within the diffuse layer towards the left pole of the particle. This redistribution of the diffuse layer leads to the different results for conducting and non-conducting particle.

In the case of non-conducting particle, the surface charge cannot move. It retains its spherical symmetry. As a result the particle gains an excess negative charge at the right hand side pole and excessive positive charge at the left hand side pole. It gains a dipole moment. This dipole moment generates an external electric field, which gives rise to the colloid vibration current.

In the case of a conducting particle, the charge carriers inside the particle can follow the counter-ions of the DL that are being dragged to the left hand side pole. This means that the surface charge, or charge associated with the particle, loses its internal spherical symmetry as well as the charge of the diffuse layer. Most importantly, each element of the surface, as well as the adjacent diffuse layer, remains electro-neutral. No external electric field appears and electroacoustic effect is practically zero.

Does this mean that electroacoustics is useless for water-in-oil emulsions?

The answer is *No*.

So far we have considered a water-in-oil emulsion with the thin isolated DLs. In the water-in-oil emulsions with overlapped DLs the nature of electroacoustic effect is quite different.

Homogeneous distribution of the counter-ions eliminates polarization charges induced on the left hand side pole of the particles by the liquid motion. The electroacoustic effect is related simply to the displacement current of the oscillating motion of the particle surface charges.

There is only one electroacoustic theory that takes into account DLs overlap. It was created in the year 2002 by Shilov et al. [7]. It yields the following expression for the dynamic mobility:

$$\mu_d = \frac{2\sigma a}{3} \frac{\rho_m}{\rho_s \eta \Omega + i\omega(1-\varphi)(2a^2/9)\rho_p \rho_m} \quad (\text{A.8})$$

where  $\sigma$  is surface charge density,  $\Omega$  a hydrodynamic drag coefficient, and  $\omega$  the ultrasound frequency.

It is seen that there are no electrodynamic parameters for either the particles or the media are involved in this expression. This leads us to the conclusion that, in the case of overlapped DLs, water-in-oil emulsions generate an electroacoustic signal in a similar manner as non-conducting particles.

According to the Shilov's theory, in the case of overlapped DLs, we can calculate the surface charge of the particles from the dynamic mobility knowing nothing about the relevant ions or even the ionic strength. We know of

only one other electrokinetic theory with a similar level of simplicity—Smoluchowski theory.

This general nature of Shilov's theory is especially important for non-polar liquids. We have currently very little knowledge and few means to collect information about ions in these liquids. We have published recently a paper that addresses this issue in more detail [15].

The calculation of  $\zeta$ -potential does require information of the ions, because it includes Debye length

$$\sigma = \frac{1}{3} \frac{RT}{F} \frac{1-\varphi}{\varphi} \varepsilon_0 \varepsilon_m a \kappa^2 \sin h \frac{F\zeta}{RT} \quad (\text{A.9})$$

where  $T$  is the absolute temperature,  $F$  the Faraday constant,  $R$  a gas constant.

This simple analysis leads us to the following conclusions:

- water-in-oil emulsion with isolated DLs should not generate any electroacoustic signal;
- measurable electroacoustic signal generated by water-in-oil emulsion indicates that DLs are overlapped.

## References

- [1] J.T. Davies, E.K. Rideal, Disperse systems and adhesion, in: H. Willmer (Ed.), *Interfacial Phenomena*, 1st ed., Academic Press, NY, 1961, pp. 343–450.
- [2] J.C. Lopez-Montilla, P.E. Herrera-Morales, S. Pandey, D.O. Shah, Spontaneous emulsification: mechanisms, physicochemical aspects, modeling and applications, *J. Dispers. Sci. Technol.* 23 (1–3) (2002) 219–268.
- [3] H. Kunieda, Y. Fukui, H. Uchiyama, C. Solans, Spontaneous formation of highly concentrated water-in-oil emulsions, *Langmuir* 12 (9) (1996) 2136–2140.
- [4] A.S. Dukhin, P.J. Goetz, *Ultrasound for Characterizing Colloids*, Elsevier, 2002.
- [5] O.B. Ho, Surfactant stabilized emulsions from an electrokinetic perspective, in: A.V. Delgado (Ed.), *Interfacial Electrokinetics and Electrophoresis*, Marcel Dekker, 2002, pp. 869–892.
- [6] K.G. Marinova, R.G. Alargova, N.D. Denkov, O.D. Velev, D.N. Petsev, I.B. Ivanov, R.P. Borwankar, Charging of oil-water interfaces due to spontaneous adsorption of hydroxyl ions, *Langmuir* 12 (1996) 2045–2051.
- [7] V.N. Shilov, Yu.B. Borkovskaja, A.S. Dukhin, Electroacoustic theory for concentrated colloids with arbitrary  $\kappa_a$ : nano-colloids, non-aqueous colloids, *JCIS* 277 (2004) 347–358.
- [8] A. Kitahara, Nonaqueous systems, in: A. Kitahara, A. Watanabe (Eds.), *Electrical Phenomena at Interfaces*, Marcel Dekker, 1984.
- [9] Ph.C. van der Hoeven, J. Lyklema, Electrostatic stabilization of suspensions in non-aqueous media, *Adv. Colloid Interf. Sci.* 42 (1992) 205–277.
- [10] I.D. Morrison, Electrical charges in non-aqueous media, *Colloids Surf. A* 71 (1993) 1–37.
- [11] R.W. O'Brien, T.A. Wade, M.L. Carasso, R.J. Hunter, W.N. Rowlands, J.K. Beattie, Electroacoustic determination of droplet size and zeta potential in concentrated emulsions, *JCIS* (1996).
- [12] A.J. Babchin, R.S. Chow, R.P. Sawatzky, Electrokinetic measurements by electroacoustic methods, *Adv. Colloid Interf. Sci.* 30 (1989) 111.

- 798 [13] A.S. Dukhin, V.N. Shilov, H. Ohshima, P.J. Goetz, Electroacoustics  
799 phenomena in concentrated dispersions new theory and CVI exper-  
800 iment, *Langmuir* 15 (20) (1999) 6692–6706. 803
- 801 [14] A.S. Dukhin, V.N. Shilov, H. Ohshima, P.J. Goetz, Electroacoustics  
802 phenomena in concentrated dispersions effect of the surface conduc-  
tivity, *Langmuir* 16 (2000) 2615–2620. 804
- [15] A.S. Dukhin, P.J. Goetz, *Colloids Surf.*, submitted for publi-  
cation. 805
- [16] J. Rudin, D.T. Wasan, Interfacial turbulence and spontaneous emulsi-  
fication in alkali–acidic oil systems, *Chem. Eng. Sci.* 48 (12) (1993)  
2225–2238. 806  
807

UNCORRECTED PROOF